Rhenium and technetium complexes bearing quinazoline derivatives: progress towards a ^{99m}Tc biomarker for EGFR-TK imaging†

Célia Fernandes,[a] Isabel C. Santos,[a] I. Santos,*[a] Hans-Jurgen Pietzsch,[b] Jens-Uwe Kunstler,[b] Werner Kraus,[c] Ana Rey,[d] Nikos Margaritis,[e] Athanasia Bourkoula,[e] Aris Chiotellis,[e] Maria Paravatou-Petsotas[e] and Ioannis Pirmettis[e]

Received 4th February 2008, Accepted 1st April 2008
First published as an Advance Article on the web 13th May 2008
DOI: 10.1039/b802021c

The quinazoline derivatives (3-chloro-4-fluorophenyl)quinazoline-4,6-diamine (**2**) and (3-bromophenyl)quinazoline-4,6-diamine (**3**) were labelled with ^{99m}Tc using the "4 + 1" mixed-ligand system [Tc(NS_3)(CN-R)] and the tricarbonyl moiety *fac*-[Tc($CO)_3$]$^+$. In the "4 + 1" approach the technetium(III) is stabilized by a monodentate isocyanide bearing a quinazoline fragment (**L^1**, **L^2**) and by the tetradentate tripodal ligand tris(2-mercaptoethyl)-amine (NS_3). In the "4 + 1" approach, ^{99m}Tc-labelling was performed in a two-step procedure, the complexes [Tc(NS_3)(**L^1**)] (**7a**) and [Tc(NS_3)(**L^2**)] (**8a**) being obtained in about 50–70% yield. In the tricarbonyl approach, the *fac*-[Tc($CO)_3$]$^+$ unit is anchored by two different monoanionic chelators bearing the quinazoline derivatives (3-chloro-4-fluorophenyl)quinazoline-4,6-diamine (**2**) and (3-bromophenyl)quinazoline-4,6-diamine (**3**). Both chelators have a N_2O donor atom set, but one contains a pyrazolyl ring (**L^5**H) and the other contains a pyridine unit (**L^6**H). In both cases the conjugation of the quinazoline to the chelator was done through the secondary amine of the potentially tridentate and monoanionic chelators, the corresponding ^{99m}Tc-complexes (**10a**, **11a**) being obtained in quantitative yield. The identities of the ^{99m}Tc-labelled quinazolines (**7a**, **8a**, **10a**, **11a**) were confirmed by comparison with the HPLC profiles of the analogous Re compounds (**7**, **8**, **10**, **11**). All these Re complexes were characterized by NMR and IR spectroscopy, elemental analysis and in some cases by MS and X-ray diffraction analysis. *In vitro* studies indicate that the quinazoline fragments, after conjugation to the cyano group (**L^1**, **L^2**) or to the pyrazolyl containing chelator (**L^5**H), as well as the corresponding Re complexes (**7**, **8**, **10**) inhibit significantly the EGFR autophosphorylation and also inhibit A431 cell growth. These two effects were also found for the pyridine-containing chelator (**L^6**H) and corresponding Re complex (**11**), although to a lesser extent.

Introduction

The human epidermal growth factor (HER) family consists of four distinct but closely related transmembrane receptors, namely EGFR or HER1, HER2, HER3 and HER4. From all these receptors it is known that EGFR is over-expressed and/or dysregulated in several solid tumors. These receptors normally possess an extracellular ligand binding domain, a transmembrane region and an intracellular cytoplasmatic domain with tyrosine kinase activity.[1–3] The most important endogenous stimulatory ligands for EGFRs are epidermal growth factor (EGF) and transforming growth factor α (TGFα). After ligand binding, the receptor undergoes dimerisation, forming either homodimers or heterodimers, followed by internalisation of the receptor–ligand complex, which induces tyrosine kinase catalytic activity leading to autophosphorylation in several tyrosines within the receptor's carboxyl-terminal tail.[4] These events will trigger a signalling network that results for example in tumour cell proliferation, angiogenesis and protection from apoptosis.

A better understanding of EGFR and of its ligands has motivated research on new therapeutic strategies for targeting EGFR and has been reviewed in several papers.[2,4–9] The most studied compounds have been monoclonal antibodies or tyrosine kinase inhibitors (EGFR-TKI). Monoclonal antibodies act in the extracellular domain of the receptor and tyrosine kinase inhibitors bind to the intracellular tyrosine kinase region, competing with ATP (adenosine triphosphate). Several classes of tyrosine kinase inhibitors have been reported and, among them, the most potent, selective and approved are iressa/gefitinib and tarceva/erlotinib (Chart 1).

Tumour imaging of EGFR receptors has been attempted with monoclonal antibodies or with EGF analogues labelled with ^{99m}Tc, ^{111}In or ^{131}I.[9] Recently, there has also been growing interest in the use of radioprobes based on tyrosine kinase inhibitors.

[a]*Departamento de Química, ITN, Estrada Nacional 10, 2686-953, Sacavém Codex, Portugal. E-mail: isantos@itn.pt*
[b]*Institute of Radiopharmacy, Forschungszentrum Dresden-Rossendorf, P.O.B. 510 119, 01314, Dresden, Germany*
[c]*Federal Institute for Materials Research and Testing (BAM), 12205, Berlin, Germany*
[d]*Radiochemistry Department, Faculty of Chemistry, Universidad de la Republica, Montevideo, Uruguay*
[e]*Institute of Radioisotopes - Radiodiagnostic Products, National Centre for Scientific Research "Demokritos", 15310, Athens, Greece*

† CCDC reference numbers 676393 (for **8**) and 676394 (for **9**). For crystallographic data in CIF or other electronic format see DOI: 10.1039/b802021c

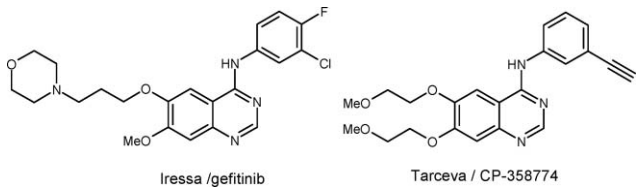

Chart 1

These radioprobes would be very helpful in the selection of patients for TKI therapy and to monitor their response to personalized cancer management.[4–9] Particularly, those from the 4-anilinoquinazoline class were labelled with short-lived positron emitters, like ^{11}C,[10–17] ^{18}F[18–21] and ^{124}I,[22–23] but up to now, to the best of our knowledge, no labelling has been attempted with ^{99m}Tc.[9] However, the widespread availability of single-photon-emission tomography (SPECT) facilities in comparison with PET, the worldwide availability of ^{99}Mo–^{99m}Tc generators and the almost ideal properties of ^{99m}Tc for SPECT imaging still justify the interest in ^{99m}Tc biocomplexes specific for EGFR-TK, as an alternative to PET radioligands. In this manuscript, we describe our attempts to label two quinazoline derivatives with the metal fragments $[M(NS_3)(CNR)]$ and *fac*-$[M(CO)_3]^+$ (M = Re, ^{99m}Tc). One of the quinazoline derivatives is related to PD 153035 (4-[(3-bromophenyl)amino]-6,7-dimethyoxyquinazoline) and the other to the recently approved gefitinib.[9] We will present the synthesis and characterization of the quinazoline analogues, their conjugation to tailor-made ligands for the two metal cores explored and the synthesis and characterization of the corresponding Re and Tc complexes. The inhibition of autophosphorylation and cell growth by the compounds described in this work is also reported.

Experimental

Unless otherwise stated, all chemicals were of reagent grade and were used without further purification. NMR (^1H, ^{13}C and ^{19}F) spectra were recorded on Varian Unity 300, 400 or 500 MHz spectrometers. The NMR spectra were run at room temperature. ^1H and ^{13}C chemical shifts are reported relative to residual solvent signals or TMS as reference. Mass spectrometric measurements were performed with a Micromass Tandem Quadropole Mass Spectrometer (Quadro LC) operating in the MS mode. Mass spectral data were recorded in the positive ESI mode. About 10^{-4} mol of the sample dissolved in 1.0 mL of methanol or acetonitrile were injected at a flow rate of 5 mL min^{-1}. Elemental analyses were performed on a LECO Elemental Analyzer CHNS-932 or on a EA 1110 CE Instrument automatic analyser. IR spectra were recorded on a FTIR spectrometer IR 2000 (Perkin-Elmer) or on a Bruker Tensor 27 spectrometer, using KBr pellets.

Chemical reactions were monitored by thin-layer chromatography (TLC) on Merck plates precoated with silica gel 60 F_{254}. Column chromatography was performed in silica gel 60 (Merck). Sodium pertechnetate, $Na[^{99m}TcO_4]$, was eluted from a commercial $^{99}Mo/^{99m}Tc$ generator (MDS Nordion S.A., Belgium or Mallinckrodt), using 0.9% saline solution. High performance liquid chromatography (HPLC) analysis of the ligands, Re and ^{99m}Tc complexes was performed on a Perkin Elmer system equipped with a biocompatible quaternary pump (LC 200), a tunable UV/Vis detector (LC 290, Perkin Elmer) and a radiometric detector (LB 509, Berthold). Ligands and the Re complexes were detected by UV detection at 254 nm. Separations were achieved on a reversed phase (RP) Hypersil ODS column (4.0 × 250 mm, 10 μm) eluted with a binary gradient system with a flow rate of 1.0 mL min^{-1}. Mobile phase A: aqueous 0.5% TFA solution, mobile phase B: 0.1% TFA solution in acetonitrile; method: t = 0–3 min, 0% B; 3–3.1 min, 0–25% B; 3.1–9 min, 25% B; 9–9.1 min, 25–34% B; 9.1–20 min, 34–100% B; 20–25 min, 100% B; 25–25.1 min, 100–0% B; 25.1–30 min, 0% B. The ^{99m}Tc complexes were also analysed by TLC using a mixture of methanol (95%)–HCl 6 N (5%).

The compounds *N*-(2-bromoethyl)-3,5-dimethylpyrazole,[24] picolinamine-*N*,*N*-diacetic acid (PADA),[25] *N*,*N*-bis[2-oxo-3-oxazolidinyl]phosphorodiamidic chloride (BOP-Cl),[26] 6-amino-4-[(3-chloro-4-fluorophenyl)amino]quinazoline (**2**),[27] 6-amino-4-[(3-bromophenyl)amino]quinazoline (**3**),[28] the tetradentate tripodal ligand tris(2-mercaptoethyl)amine (NS_3) and the rhenium starting complexes $[ReNS_3(PMe_2Ph)]$ and $[NEt_4]_2[Re(Br)_3(CO)_3]$ were prepared as reported elsewhere.[29,30] Tris(2-mercaptoethyl)amine was isolated and applied as the oxalate. The radioactive precursor *fac*-$[^{99m}Tc(CO)_3(H_2O)_3]^+$ was prepared using an IsoLink kit (Malinckrodt), according to the manufacturers.

Synthesis and characterization of *N*-{4-[(3-chloro-4-fluorophenyl)amino]quinazolin-6-yl}-3-isocyanopropanamide (L^1) and *N*-{4-[(3-bromophenyl)amino]quinazolin-6-yl}-3-isocyanopropanamide (L^2)

1. Synthesis of *N*-formyl β-alanin (1). β-Alanin (10 g, 112 mmol) was dissolved in a mixture of 80 mL of formic acid and 50 mL of acetic anhydride and heated under reflux for 6 h. After removal of the solvent, the remaining white powder was washed with diethyl ether and recrystallized from 2-propanol, yielding a white powder: yield. 45%. Elem. Anal. ($C_4H_7NO_3$ MW: 117.10) Calc. C, 41.03%, H, 6.03%, N, 11.96%; Found C, 41.23%, H, 5.86%, N, 12.12%.

2. General procedure for preparation of *N*-formylquinazolines 4 and 5. 80 mg (640 μmol) of diisopropylethyl amine and 205 mg (640 μmol) of *O*-(benzotriazol-1-yl)-*N*,*N*,*N*′,*N*′-tetramethyluronium tetrafluoroborate (TBTU) were added to 78 mg (670 μmol) of **1**, dissolved in 3 mL of *N*-methyl-2-pyrrolidone. After stirring at room temperature for 5 min, 536 μmol of **2** or **3**, dissolved in 4 mL of *N*-methyl-2-pyrrolidone, was added in one step. The yellow reaction mixture was stirred at room temperature for 24 h. After removal of the solvent the product was purified by column chromatography on silica gel 60 using a mixture of chloroform–methanol–25% ammonia (80 : 60 : 0.2).

N-{*4-[(3-Chloro-4-fluorophenyl)amino]quinazolin-6-yl*}-N^3-*formyl alaninamide* (***4***). Pale tan solid, yield 30%. MS (ES+): 388.17 $[M + H]^+$. Elem. Anal. ($C_{18}H_{15}ClFN_5O_2$ MW: 387.79) Calc. C, 55.75%, H, 3.90%, N, 18.06%; Found C, 55.46%, H, 3.78%, N, 18.27%.

N-{*4-[(3-bromophenyl)amino]quinazolin-6-yl*}-N^3-*formyl alaninamide* (***5***). Pale tan solid, yield 35%. MS (ES+): 415.20 $[M + H]^+$. Elem. Anal. ($C_{18}H_{16}BrN_5O_2$ MW: 414.26) Calc. C, 52.19%, H, 3.89%, N, 16.91%; Found C, 52.43%, H, 3.96%, N, 16.77%.

3. General procedure for preparation of isocyanides L^1 and L^2. 200 μmol of **4** or **5** was dissolved in 10 mL of anhydrous pyridine, and 70 mg (360 μmol) of *p*-toluenesulfonyl chloride was added.

After being stirred for 6 h at room temperature, the mixture was transferred into a flask filled with ice. After the ice was slowly melted, the precipitate was filtered off and washed with water until no pyridine smell was noticed. The product was purified by column chromatography on silica gel 60 using a mixture of chloroform–methanol–25% ammonia (80 : 60 : 0.2) as eluent.

***L*^{1}**. Beige solid, yield: 33%. IR (KBr, cm^{-1}): 2157 ν(–N≡C). ^{1}H NMR (400 MHz, DMSO-d_6): δ (ppm) 2.8 (2H, CH_2), 3.8 (2H, CN-CH_2), 7.4–8.7 (7H_{arom}), 9.9 (NH), 10.4 (NH-C(O)). Elem. Anal. ($C_{18}H_{13}ClFN_5O$ MW: 369.78) Calc. C, 58.47%, H, 3.54%, N, 18.94%; Found C, 58.61%, H, 3.86%, N, 18.77%.

***L*^{2}**. Beige solid, yield: 37%. IR (KBr, cm^{-1}): 2155 ν(–N≡C). ^{1}H NMR (400 MHz, DMSO-d_6): δ (ppm) 2.8 (2H, CH_2), 3.8 (2H, CN-CH_2), 7.3–8.7 (8H_{arom}), 9.9 (NH), 10.5 (NH-C(O)). Elem. Anal. ($C_{18}H_{14}BrN_5O$ MW: 396.24) Calc. C, 54.56%, H, 3.56%, N, 17.67%; Found C, 54.91%, H, 3.84%, N, 17.91%.

***N*-{4-[(3-Chloro-4-fluorophenyl)amino]quinazoline-6-yl}-3-bromopropionamide (6).** 3-Bromopropanoyl chloride (446 mg, 2.6 mmol) was added slowly to a solution of 6-amino-4-[(3-chloro-4-fluorophenyl)amino]quinazoline (**2**) (342 mg, 1.2 mmol) in dry acetone (15 mL). A yellow precipitate formed and the reaction mixture was left under stirring for 2 h. The precipitate was separated by filtration and dried under reduced pressure yielding **6** as a yellow solid. Yield: (394 mg, 79%). ^{1}H NMR ($(CD_3)_2SO$) δ (ppm): 3.09 (t, 2H, -CH_2-CH_2-Br); 3.78 (t, 2H, -CH_2-CH_2-Br); 7.55 (t, 1H, H-5′, J = 8.7Hz); 7.65 (m, 3H, H-6′); 7.91 (d, 1H, H-8); 7.96 (m, 1H + 1H, H-2′, H-7); 8.8 (s, 1H, H-2); 9.02 (s, 1H, H-5); 10.76 (s, 1H, N*H*), 11.46 (s,1H,CON*H*). ^{1}H NMR (CD_3OD) δ (ppm): 2.96 (t, 2H, -CH_2-CH_2-Br); 3.93 (t, 2H, -CH_2-CH_2-Br); 7.37 (t, 1H, arom); 7.71–7.66 (m, 3H, arom); 8.04–7.84 (m, 1H, arom); 8.76 (s, 1H, arom); 9.01 (s, 1H, arom). ^{13}C NMR (CD_3OD) δ (ppm): 171.5 (*C*ONH), 161.7, 157.9 (d, J_{F-C} 247 Hz), 150.8, 140.7, 136.3, 134.7, 130.7, 128.4, 126.4, 126.5, 117.9 (d, J_{F-C} 22.5 Hz), 115.6, 113.5, 40.8 (CH_2), 27.8 (CH_2). IR (KBr) (cm^{-1}): 1681.32 (vs); 1498.64 (s); 1446.54 (s); 1205.33 (vs). HPLC r.t. = 10.6 min.

Synthesis and characterization of [2-(3,5-dimethylpyrazol-1-yl)ethylamino]acetic acid (L^{3}H) and {bis[2-(3,5-dimethylpyrazol-1-yl)ethyl]amino}acetic acid (L^{4}H)

1.4 g (18.5 mmol) of glycine in H_2O (15 mL) was added to a solution of *N*-(2-bromoethyl)-3,5-dimethylpyrazole (0.745 g, 3.7 mmol) in ethanol (20 mL) and the pH adjusted to 10 by adding 5 M NaOH. The mixture was refluxed during four days, maintaining the pH in the range 8–10, by adding small amounts of 5 M NaOH. After removing the solvent under vacuum, the crude was analyzed by NMR spectroscopy. Based on the NMR data, the crude contains approximately 80% of **L^{3}H** and 20% of **L^{4}H**. This mixture was applied on a silica gel chromatography column, and **L^{3}H** and **L^{4}H** were separated using as solvent MeOH–25% NH_4OH–$CHCl_3$ and a gradient from 10 : 2 : 88 to 98 : 2 : 0.

L^{3}H. Yield 400 mg, 2.1 mmol; 56%, ^{1}H NMR [δ, ppm, D_2O]: 5.84 (s, 1H, H(4)pz), 4.21 (t, 2H, CH_2), 3.43 (s, 2H, CH_2CO), 3.31 (t, 2H, CH_2), 2.11 (s, 3H, CH_3), 2.02 (s, 3H, CH_3). ^{13}C NMR [δ, ppm, D_2O (dioxane as reference)]: 173.7 (COOH), 152.7 (C(3)pz), 144.6 (C(5)pz), 108.7 (C(4)pz), 51.9 (CH_2), 49.4 (CH_2), 46.7 (CH_2), 14.9 (CH_3), 12.6 (CH_3). IR (KBr, cm^{-1}): 1601.8 (ν(C=O)). Elem. Anal. ($C_9H_{14}O_2N_3Na$ MW: 219.22) Calc: C, 49.31%, H, 6.44%, N, 19.17%; Found: C, 49.36%, H, 8.08%, N, 18.51%.

L^{4}H. Yield 92 mg, 0.29 mmol, 16%: ^{1}H NMR [δ, ppm, D_2O]: 5.87 (s, 2H, H(4)pz), 4.08 (t, 4H, CH_2), 3.34 (s, 2H, CH_2CO), 3.18 (t, 4H, CH_2), 2.14 (s, 6H, CH_3), 2.06 (s, 6H, CH_3). ^{13}C NMR [δ, ppm, D_2O]: 174.8 (COO), 151.5 (C(3)pz), 144.1 (C(5)pz), 108.0 (C(4)pz), 58.9 (CH_2), 55.9 (CH_2), 45.6 (CH_2), 14.3 (CH_3), 12.1 (CH_3). Elem. Anal. ($C_{16}H_{25}O_2N_5$ MW: 319.41) Calc: C, 60.17%, H, 7.89%, N, 21.93%; Found: C, 60.33%, H, 8.05%, N, 21.54%.

Synthesis and characterization of L^{5}H

50 mg (0.25 mmol) of **L^{3}H** in 2 mL H_2O reacted with 100 mg (0.24 mmol) of **6** in THF (3 mL). The pH was adjusted to 8–10 by adding NaOH 5 M. The mixture was refluxed and the pH controlled and adjusted to be maintained between 8 and 10. The reaction mixture was vacuum dried and the solid purified by silica gel column chromatography, using as solvent MeOH–25% NH_4OH–$CHCl_3$ and a gradient from 10 : 2 : 88 to 98 : 2 : 0. Yield 45mg, 0.08 mmol, 34%, ^{1}H NMR [δ, ppm, CD_3OD]: 8.70 (d, 1H, H(5)), 8.56 (s, 1H, H(2)), 8.00 (d, 1H, H(7)), 7.82 (dd, 1H H(2′)), 7.67–7.74 (m, 2H, H(8), H(6′)), 7.28 (t, 1H, (H5′)), 5.69 (s, 1H, H(4)pz), 4.24 (t, 2H, CH_2), 3.72 (s, 2H, CH_2COOH), 3.31–3.39 (m, 4H, 2CH_2), 2.78 (t, 2H, CH_2) 2.23 (s 3H, Me), 2.06 (s, 3H, Me). ^{13}C NMR [δ, ppm, CD_3OD]: 177.3 (CONH), 172.9 (COO), 159.5, 156.1 (d, J_{F-H} 240 Hz), 154.3 (C(3), pz), 148.8, 147.0 (C(5), pz), 141.7, 138.9, 137.3, 129.3, 128.1, 126.01, 124.2 (d), 121.3 (d, J_{F-C} 18.5 Hz), 117.4 (d, J_{F-C} 22.2 Hz), 116.6, 112.6, 106.0 (C(4), pz), 59.5 (CH_2), 54.4 (CH_2), 51.7 (CH_2), 46.7 (CH_2), 35.2 (CH_2), 13.3 (CH_3-pz), 11.1 (CH_3-pz). RP-HPLC (UV/Vis detection, 254 nm) retention time: 16.0 min.

Synthesis and characterization of ({[(*N*-(3-bromophenyl)amino)quinazolin-6-ylcarbamoyl]methyl}pyridin-2-ylmethylamino)acetic acid (L^{6}H)

Picolylaminodiacetic acid (PADA) (0.897 g, 4 mmol) was dissolved in anhydrous THF (20 mL) with the addition of Et_3N (1.7 mL, 12 mmol). To this solution, *N*,*N*-bis[2-oxo-3-oxazolidinyl]phosphorodiamidic chloride (1.018 g, 4 mmol) was added and the resulting mixture was stirred vigorously under nitrogen in a water bath at 20 °C for 1 h and then filtered. 5.5 mL of the filtrate, which contains 1 mmol of the picolylaminodiacetic anhydride, was added to a solution of 6-amino-4-[(3-bromophenyl)amino]quinazoline (**3**) (0.315 g, 1 mmol) dissolved in THF (5 mL). The solution was stirred under nitrogen for 2 h and then concentrated under reduced pressure. The residue was purified by column chromatography on silica gel using a mixture of CH_2Cl_2–EtOH 5 : 1 to give **L^{6}H** (0.350 g, 67%) as pale yellow solid. Elem. Anal. ($C_{24}H_{21}BrN_6O_3$) Calc: C, 55.29%, H, 4.06%, N, 16.12%. Found: C, 54.95%, H, 4.12%, N, 16.01%; δ_H (500 MHz; $(CH_3)_2SO$; Me_4Si) 10.82 (1H, s, CON*H*), 9.97 (1H, s, N*H*), 8.70 (1H, s, H(5)), 8.61 (1H, d, H(6)py), 8.58 (1H, s, H(2)), 8.18 (1H, s, H(2′)), 8.08 (1H, d, H(7)), 7.87 (1H, d, H(6′)), 7.81 (1H, H(8)), 7.79 (1H, H(4)py), 7.50 (1H, d, H(3)py), 7.35 (1H, t, H(5′)), 7.30 (1H, H(4′)), 7.29 (1H, H(5)py), 4.04 (2H, s, py-CH_2N), 3.63 (2H, s, NCH_2CON), 3.53 (2H, s, NCH_2COO); δ_C (125 MHz, $(CH_3)_2SO$) 172.9 (COOH), 169.9 (N-CH_2*C*ON), 158.3 (C2 py), 157.3 (C4),

153.0 (C2), 149.2 (C6 py), 146.6 (C9), 141.2 (C3′), 137.0 (C4 py), 136.6 (C6), 130.4 (C5′), 128.6 (C8), 126.8 (C7), 125.9 (C4′), 124.3 (C2′), 123.2 (C3 py), 122.6 (C5 py), 121.1 (C1′), 120.9 (C6′), 115.5 (C10), 111.4 (C5), 59.5 (py-CH_2-N), 58.3 (N-CH_2-CON), 55.0 (NCH_2-COOH). The HPLC retention time (UV detection at 254 nm) was 15.0 min.

General procedure for preparation of rhenium complexes 7 and 8

7 mg (14 μmol) of [$ReNS_3(PMe_2Ph)$] was dissolved in 2 mL of chloroform. After addition of 14 μmol of isocyanide **L**[1] or **L**[2] the reaction mixture was refluxed for 1 h. After washing the reaction mixture twice with water the solvent was evaporated and the complex was purified by column chromatography on silica gel 60 using a mixture of chloroform–methanol–25% ammonia (80 : 60 : 0.2) as eluent. Recrystallization of the crude complexes from chloroform–methanol (50 : 50, v/v) yielded complexes **7** and **8**.

[Re(NS_3)(CN-quinazoline-Cl,F)] (7). Olive-green crystals, yield: 90%. MS (ES+): 751.45 $[M + H]^+$. IR (KBr, cm^{-1}): 1958 (v br) ν(–N≡C). ^{1}H NMR: (DMSO-d_6): δ (ppm) 2.8 (1H), 2.5–3.2 (12H, N(CH_2CH_2S)$_3$, 5.2 (2H, CN-CH_2), 7.2–8.7 (7H_{arom}), 9.9 (NH), 10.3 (NH-C(O)). HPLC (UV/Vis detection, 254 nm) retention time: 12.5 min. Elem. Anal. ($C_{24}H_{25}ClFN_6OReS_3$ MW: 750.35) Calc. C, 38.42%, H, 3.36%, N, 11.20%; S, 12.82% Found C, 38.75%, H, 3.54%, N, 11.39%, S, 13.02%.

[Re(NS_3)(CN-quinazoline-Br)] (8). Olive-green crystals, yield: 94%. MS (ES+): 777.22 $[M + H]^+$. IR (KBr, cm^{-1}): 1953 (v br) ν(–N≡C). ^{1}H NMR: (DMSO-d_6): δ (ppm) 2.8–3.2 (1H), 2.5–3.2 (12H, N(CH_2CH_2S)$_3$, 5.1 (2H, CN-CH_2), 7.2–8.8 (8H_{arom}), 9.9 (NH), 10.4 (NH-C(O)). HPLC (UV/Vis detection, 254 nm) retention time: 12.8 min. Elem. Anal. ($C_{24}H_{26}BrN_6OReS_3$ MW: 776.81) Calc. C, 37.11%, H, 3.37%, N, 10.82%; S, 12.38%; Found C, 36.95%, H, 3.54%, N, 11.10%, S, 12. 61%.

Synthesis of Re(I) complexes 9–11

$[NEt_4]_2[Re(Br)_3(CO)_3]$ (58 mg, 0.08 mmol) was reacted with **L**[3]H (1 : 2 molar ratio) in H_2O, with **L**[5]H (1 : 1 molar ratio) in MeOH–H_2O for 3 h at 70 °C and with **L**[6]H (1 : 1 molar ratio) in refluxing MeOH for 2 h. The complexes **9** and **10** precipitate as white solids from the aqueous solutions upon concentration and cooling, while **11** was obtained after evaporation of the solvent and recrystallization from methanol–dichloromethane (75 : 25, v/v).

9. Yield 29.8 mg, 0.06 mmol, 80%. IR (KBr, cm^{-1}): 2021, 1883 (very broad), 1627 (ν(C=O)). ^{1}H NMR [δ, ppm, CD_3OD]: 6.85 (m, 1H, NH), 6.13 (s, 1H, H(4)pz), 4.43 (d, m, 1H, CH_2), 4.10 (m, 1H, CH_2), 3.61 (dd, 1H, CH_2), 3.53–3.45 (m, 2H, CH_2), 2.46 (s, 3H, CH_3-pz), 2.30 (s, 3H, CH_3-pz), 2.26 (m, 1H CH_2). ^{13}C NMR [δ, ppm, $CDCl_3$]: 196.4 (CO), 196.2 (CO), 195.8 (CO), 182.8 (COO), 154.8 (C(3)pz), 144.7 (C(5)pz), 108.5 (C(4)pz), 56.6 (CH_2), 51.9 (CH_2), 47.8 (CH_2), 15.5 (CH_3-pz), 11.4 (CH_3-pz). HPLC (UV/Vis detection, 254 nm) retention time: 15.9 min. Elem. Anal. ($C_{12}O_{15}N_3H_{14}Re$ MW: 466,47) Calc. C, 30.90%; H, 3.00%; N, 9.01%; Found: C, 30.04%; H, 2.82%; N, 8.70%.

10. Yield 26 mg, 0.03 mmol, 42%. ^{1}H- NMR [δ, ppm, $(Me)_2SO$]: 10.46 (s, 1H, NH(C=O)), 9.95 (s, 1H, NH), 8.77 (d, 1H, H(5)), 8.55 (s, 1H, H(2)), 8.10 (m, 1H, H(7)), 7.77 (m, 3H, H(8), H(6′), H(2′)), 7.43 (t, 1H, (H5′)), 6.22 (s, 1H, H(4)pz), 4.22 (m, 2H, CH_2), 3.90 (m, 1H, CH_2), 3.80 (m, 1H, CH_2), 3.64 (d, 1H, CH_2COOH), 3.47(d, 1H, CH_2COOH), 2.89 (m, 4H, 2CH_2), 2.41 (s 3H, Me), 2.30 (s, 3H, Me). ^{13}C NMR [δ, ppm, $(Me)_2SO$]: 196.5 (CO), 195.4 (CO), 194.9 (CO), 177.1 (CONH), 169.1 (COO), 157.4, 153.4 (d, J_{F-C} 240 Hz), 153.0 (C(3), pz), 152.6, 146.3, 143.7 (C(5), pz), 136.7, 136.6, 128.5, 127.0, 124.0, 123.0 (d, J_{F-C} 21.6), 118.9 (d), 116.5 (d, J_{F-C} 21.6Hz), 115.3, 111.6, 107.5 (C(4), pz), 62.6 (CH_2), 60.6 (CH_2), 55.3 (CH_2), 45.3 (CH_2), 30.5 (CH_2), 15.4 (CH_3-pz), 11.1 (CH_3-pz). IR (KBr, cm^{-1}): 2024 (s), 1917 (sh), 1892 (s, br), (1701), (1645), (1616). HPLC (UV/Vis detection 254 nm) retention time: 19.4 min. Elem. Anal. ($C_{29}H_{26}ClFO_6N_7Re.2H_2O$; MW: 845.26) Calc: C, 41.21%, H, 3.58%, N, 11.60%; Found: C, 41.15%, H, 3.07%, N, 10.78%.

11. Yield 65 mg, 82%. ν_{max}(KBr)/cm^{-1} 2021 (s, C≡O), 1917 (s, C≡O), 1871 (s, C≡O), 1621 (ν(C=O)). δ_H (500 MHz; $(CH_3)_2SO$; Me_4Si) 10.68 (1H, s, CON*H*), 10.03 (1H, s, N*H*), 8.79 (1H, d, H(6)py), 8.77 (1H, s, H(5)), 8.61 (1H, s, H(2)), 8.16 (1H, s, H(2′)), 8.15 (1H, t br, H(4)py), 7.92 (1H, d, H(7)), 7.87 (1H, m, H(6′)), 7.85 (1H, m, H(8)), 7.84 (1H, m, H(3)py), 7.60 (1H, t, H(5)py), 7.36 (1H, t, H(5′)), 7.31 (1H, d, H(4′)), 5.30 (1H, d, *J* 16.2 Hz, pyCH_2N), 4.78 (1H, d, *J* 16.2 Hz, pyCH_2N), 4.78 (1H, d, *J* 16.2 Hz, NCH_2CON), 4.55 (1H, d, *J* 16.2 Hz NCH_2CON), 4.17 (1H, d, *J* 17.0 Hz, NCH_2COO), 3.82 (1H, d, *J* 17.0 Hz, NCH_2COO); δ_C (125 MHz, $(CH_3)_2SO$) 197.2 (Re-*C*O), 196.8 (Re-*C*O), 194.9 (Re-*C*O), 179.0 (-*C*OORe), 166.9 (N-CH_2*C*ON), 159.6 (C5 py), 157.3 (C4), 153.1 (C2), 151.9 (C6 py), 146.6 (C9), 141.1 (C3′), 140.6 (C4 py), 136.0 (C6), 130.3 (C5′), 128.2 (C8), 127.1 (C7), 126.0 (C4′), 125.9 (C5 py), 124.4 (C2′), 124.1 (C3 py), 121.1 (C1′), 121.0 (C6′), 115.5 (C10), 111.7 (C5), 69.4 (N-*C*H_2-CON), 68.2 (py-*C*H_2-N), 62.0 (N*C*H_2-COORe). HPLC (UV/Vis detection 254 nm) retention time: 16.9 min; Elem. Anal. ($C_{27}H_{20}BrN_6O_6Re$) Calc. C,41.02%, H, 2.55%, N, 10.63%; Found: C, 40.90%, H, 2.87%, N, 10.50%.

Crystallographic data†

Monocrystals suitable for X-ray diffraction analysis were obtained by slow concentration of solutions of **8** and **9** in chloroform–methanol (3 : 1 v/v) and in H_2O, respectively. The X-ray data were collected at room temperature on a SMART-CCD diffractometer (Siemens) (complex **8**) and on an Enraf-Nonius CAD4 diffractometer (complex **9**), using graphite monochromatized Mo-K_α radiation (λ = 0.71073 Å). Empirical absorption corrections were made. The structures were solved by direct methods. After anisotropic refinement of the non-hydrogen atoms, the hydrogen positions were calculated according to ideal geometries. Most of the calculations were carried out in the SHELXTL system with some local modifications and WINGX software package.[31] Molecular graphics were prepared using ORTEP 3.[32] A summary of the crystal data, structure solution and refinement of **8** and **9** is given in Table 1. Selected bond distances and angles are listed in Table 2.

Synthesis of the ^{99m}Tc complexes 7a and 8a

Stock solutions. EDTA solution (10 mg Na_2EDTA in 1 mL H_2O, *i.e.* 1 mg per 100 μL). Mannitol solution (50 mg mannitol in 1 mL H_2O, *i.e.* 5 mg per 100 μL).

^{99m}Tc-EDTA/mannitol. Transfer 100 μL EDTA solution and 100 μL mannitol solution into a vial (*i.e.* 1 mg Na_2EDTA, 5 mg

Table 1 Crystallographic data for complexes **8** and **9**

Empirical formula	$C_{24}H_{28}BrN_6O_2ReS_3$	$C_{48}H_{60}N_{12}O_{22}Re_4$
M/g mol^{-1}	794.81	1901.88
Temperature/K	273(2)	295(2)
Wavelength/Å	0.71073	0.71069
Cryst. syst., space group	Triclinic, $P\bar{1}$	Triclinic, $P\bar{1}$
a/Å	7.806(15)	11.3584(15)
b/Å	11.38(2)	14.756(2)
c/Å	16.23(2)	19.845(2)
α/°	91.294(19)	88.445(11)
β/°	91.37(3)	88.414(10)
γ/°	105.35(2)	76.384(12)
Volume/Å^3	1389(4)	3230.7(8)
Z	2	2
D_{cal}/Mg m^{-3}	1.900	1.934
μ/mm^{-1}	6.071	7.549
F(000)	776	1816
Crystal size/mm	0.09 × 0.07 × 0.02	0.6 × 0.26 × 0.12
Theta range/°	1.26 to 23.84	2.58 to 25.68
Limiting indices, hkl	−8/7, −12/12, −15/18	−13/0, −17/17, −24/24
Reflec. collected/unique	6811/4231 [$R_{int} = 0.0651$]	12870/12217 [$R_{int} = 0.0231$]
Completeness	98.8%	99.666%
Absorption correction	Empirical	Psi-scan
T_{max} and T_{min}	0.374 and 0.254	0.4212 and 0.1273
Refinement method	Full-matrix l.s. on F^2	Full-matrix l.s. on F^2
Data/restraints/param.	4231/3/324	12217/51/783
S on F^2	0.974	0.970
$R1$, $wR2$ [$I > 2\sigma(I)$]	0.0420, 0.1005	0.0451, 0.1009
$R1$, $wR2$ (all data)	0.0600, 0.1147	0.0758, 0.1105
$\Delta\rho$ max, min/e A^{-3}	+1.267 and −0.924	+1.601 and −1.558

Table 2 Selected bond lengths (Å) and angles (°) for compound **8** and molecule 1 of **9**

8		**9** (molecule 1)	
Re(1)–C(7)	1.944(10)	Re(1)–O(4)	2.135(6)
Re(1)–N(1)	2.223(8)	Re(1)–N(3)	2.226(7)
Re(1)–S(2)	2.234(3)	Re(1)–N(1)	2.182(7)
Re(1)–S(1)	2.241(4)	Re(1)–C(1)	1.907(10)
Re(1)–S(3)	2.249(4)	Re(1)–C(2)	1.885(11)
		Re(1)–C(3)	1.926(10)
C(7)–Re(1)–N(1)	177.3(4)	O(4)–Re(1)–N(3)	76.8(2)
C(7)–Re(1)–S(2)	94.2(3)	N(3)–Re(1)–N(1)	84.0(3)
N(1)–Re(1)–S(2)	85.9(2)	O(4)–Re(1)–N(1)	83.1(3)
C(7)–Re(1)–S(1)	96.4(3)	C(1)–Re(1)–C(2)	88.7(5)
N(1)–Re(1)–S(1)	85.8(2)	C(1)–Re(1)–C(3)	87.3(4)
S(2)–Re(1)–S(1)	119.76(14)	C(3)–Re(1)–C(2)	87.3(4)
C(7)–Re(1)–S(3)	93.2(3)	C(2)–Re(1)–O(4)	174.3(3)
N(1)–Re(1)–S(3)	84.5(3)	C(3)–Re(1)–N(3)	174.6(4)
N(1)–Re(1)–S(3)	84.5(3)	C(1)–Re(1)–N(1)	175.4(3)
S(1)–Re(1)–S(3)	118.30(12)	C(3)–Re(1)–O(4)	98.0(4)

mannitol), flush the vial with argon or nitrogen, add 20 μL $SnCl_2$ solution (0.1 mg in methanol), immediately add 300–1500 MBq $^{99m}TcO_4^-$, flush the vial with argon, let it react for 15 to 20 min at room temperature.

The radiochemical purity of ^{99m}Tc-EDTA/mannitol can be checked using TLC silica gel strips (60 W, Merck) or ITLC strips. ^{99m}Tc-EDTA/mannitol moves to the front in water and stays at the origin using acetone. The radiochemical purity is normally >90%.

The 2nd step needs to be performed immediately after the 1st step, thus the radiochemical purity of ^{99m}Tc-EDTA/mannitol can not be checked before starting step 2, only at the same time (step 1 is the synthesis of Tc(III)EDTA (see Scheme 2); step 2 is the reaction of Tc(III) with NS_3 and $\mathbf{L^1}$ or $\mathbf{L^2}$ (see Scheme 2)). It is recommended to try the preparation of ^{99m}Tc-EDTA/mannitol without continuing with step 2 until it works well.

General procedure of ^{99m}Tc complexes 7a and 8a

Add 0.3 mg of NS_3, freshly dissolved in 100 μL water, to ^{99m}Tc-EDTA/mannitol and transfer the solution to a vial containing about 0.1 mg $\mathbf{L^1}$ or $\mathbf{L^2}$, dissolved in 1 mL acetonitrile. Adjust the content of acetonitrile to half or 2/3 of the labelling mixture volume. Flush the vial with argon. Heat the solution at 60 °C for about 1 h. The labelling mixture stays clear. The radiochemical yield is about 90% (HPLC). Purification can be done by HPLC (Jupiter Proteo, 4 μm, 90 Å, 250 × 10 mm, Phenomenex; 3 mL min^{-1}; solvent A: water with 0.1% TFA (v/v), solvent B: acetonitrile with 0.1% TFA (v/v), gradient elution: 0–20 min 20 to 80% solvent B). Retention time: **7a**, 12.3 min; **8a**, 12.6 min.

Synthesis of the ^{99m}Tc complexes 9a–11a

In a nitrogen-purged glass vial, 100 μL of 10^{-4}M water solution of $\mathbf{L^3}$H (**9a**) or $\mathbf{L^5}$H (**10a**) or a methanol solution of $\mathbf{L^6}$H (**11a**) was added to 900 μL of a solution of *fac*-[^{99m}Tc$(OH_2)_3(CO)_3$]$^+$ (1–10 mCi) in PBS at pH = 7.4 (**9a**) or at pH = 5.5–6 (**10a**, **11a**) The reaction mixtures were incubated at 100 °C (**9a**, **10a**) or at 70°C for 30 min (**11a**) and then analyzed by RP-HPLC (γ detection). Retention time: **9a**, 16.0 min; **10a**, 19.6 min; **11a**, 17.2 min.

In vitro evaluation

Cell line studies. The human epidermoid carcinoma A431 cell line, kindly provided by Dr E. Mishani (Hadassah Hebrew University, Israel) were maintained in high glucose D-MEM

medium, with L-Glutamine, (PAA Laboratories GmbH) and supplemented with 10% foetal bovine serum (PAA Laboratories GmbH) and penicillin/streptomycin (PAA Laboratories GmbH) 100UI/100 μg per ml, in 5% CO_2 incubator at 37 °C. Cells were subcultured every two or three days.

Inhibition of phosphorylation. A431 cells (5×10^5) were seeded in a 6-well plate and grown to 70% confluence. Then, cells were incubated for 24 h in the presence of fresh medium without foetal bovine serum. The day after, cells were incubated in the presence of quinazoline derivatives at various final concentrations ranged from 1 to 10000 nM, for 2 h and then EGF was added (20 ng mL^{-1}) for 5 min. Then, the medium was removed, cells were washed with PBS and cell lysis buffer (50mM Tris-HCl pH 7,4, 150mM NaCl, 1% Triton X-100, 1 mM PMSF, 50 μg mL^{-1} approtinin, 2 mM sodium orthovanadate, 50 μg mL^{-1} leupeptine and 5 mM EDTA) was added. Controls consisted of wells without quinazoline derivatives and with or without EGF. The total amount of protein was estimated by a BCA assay in ELISA plates, using a BSA standard curve. A volume of lysis mixture, corresponding to 30 μg of total protein, was loaded onto polyacrylamide gel (8%), proteins were separated by electrophoresis and transferred to a PVDF membrane. For visualization of molecular weight bands, the membrane was immersed in Ponceau reagent (0.5% Ponceau in 1% acetic acid) for 5 min. The membrane was washed in H_2O, blocked overnight in TTN buffer (10mM Tris pH 7.4, 0.2% Tween 20, 170mM NaCl) with 5% milk (1% fat) and incubated for 2 h in antiphosphotyrosine antibody diluted 1/2000 (PY20, Santa Cruz Biotechnology). Then, the membrane was washed 3 times in TTN and incubated in a horseradish peroxidase-conjugated secondary anti mouse antibody diluted 1/3000, (Sigma) for 2 h and finally washed 3 times in TTN. Detection was performed using a chemiluminescent detection system according to the manufacturer's instructions (ECL kit, Amersham). Band quantification was performed using the Band leader ver. 3.00 program and the percentage of EGFR autophosphorylation inhibition was calculated.

***In vitro* growth inhibition assay.** The A431 cells were seeded in a 96-well plate at a density of 3000 cells per 100 μL per well and incubated for 24 h for attachment. The day after seeding, exponentially growing cells were incubated with various concentrations of quinazoline derivatives (ranging from 1 nM to 100 μM in 4 replicates) during 72 h. Controls consisted of wells without drugs. The medium was removed and the cells were incubated for 4 h in the presence of 1 mg mL^{-1} MTT (Sigma) in RPMI (PAA Laboratories GmbH) without phenol red at 37 °C. The MTT solution was removed and 100 mL $well^{-1}$ of isopropanol was added. After thorough mixing, absorbance of the wells was read in an ELISA reader at test and reference wavelengths of 540 and 620 nm, respectively. The mean of the optical density of different replicates of the same sample and the percentage of each value was calculated (mean of the OD of various replicates/OD of the control). The percentage of the optical density against drug concentration was plotted on a semilog chart and the IC_{50} from the dose response curve was determined.

Results and discussion

Previous studies have shown that Tc^{III} mixed-ligand complexes with tetradentate/monodentate NS_3/isonitrile coordination, [Tc(NS_3)(CN-R)], are lipophilic and stable against exchange reactions *in vivo*.[33] These "4 + 1" organometallic Tc complexes appear suitable to wrap the metal well in a molecule with receptor-binding functionality.[34,35]

The here introduced compounds contain the (3-chloro-4-fluorophenyl)quinazoline-4,6-diamine (**2**) or (3-bromophenyl)-quinazoline-4,6-diamine (**3**) moiety linked to the neutral and oxo-free technetium(III) chelate unit *via* a isocyano-modified C_3 alkyl amide. The synthesis of the isocyano-modified C3 alkyl amides, $\mathbf{L^1}$ and $\mathbf{L^2}$, involves the coupling of *N*-formyl-β-alanin (**1**) to (3-chloro-4-fluorophenyl)quinazoline-4,6-diamine (**2**) and (3-bromophenyl)quinazoline-4,6-diamine (**3**), respectively, followed by the formation of the appropriate isonitrile (Scheme 1).

In the present study rhenium complexes **7** and **8** were used as reference compounds for complete chemical characterization, identification of the ^{99m}Tc complexes (**7a** and **8a**), and for *in vitro* receptor binding assay. As can be seen in Scheme 2, after preparing the precursor complex [Re(NS_3)PMe_2Ph] the desired "4 + 1"

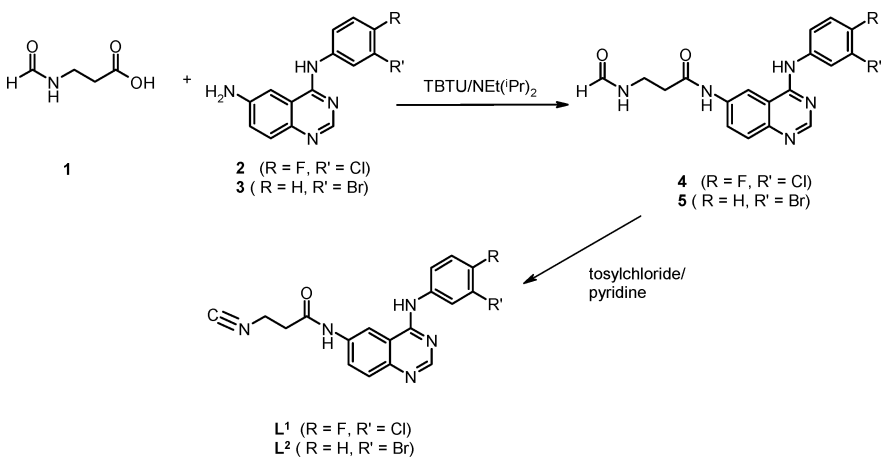

Scheme 1 Synthesis of $\mathbf{L^1}$ and $\mathbf{L^2}$.

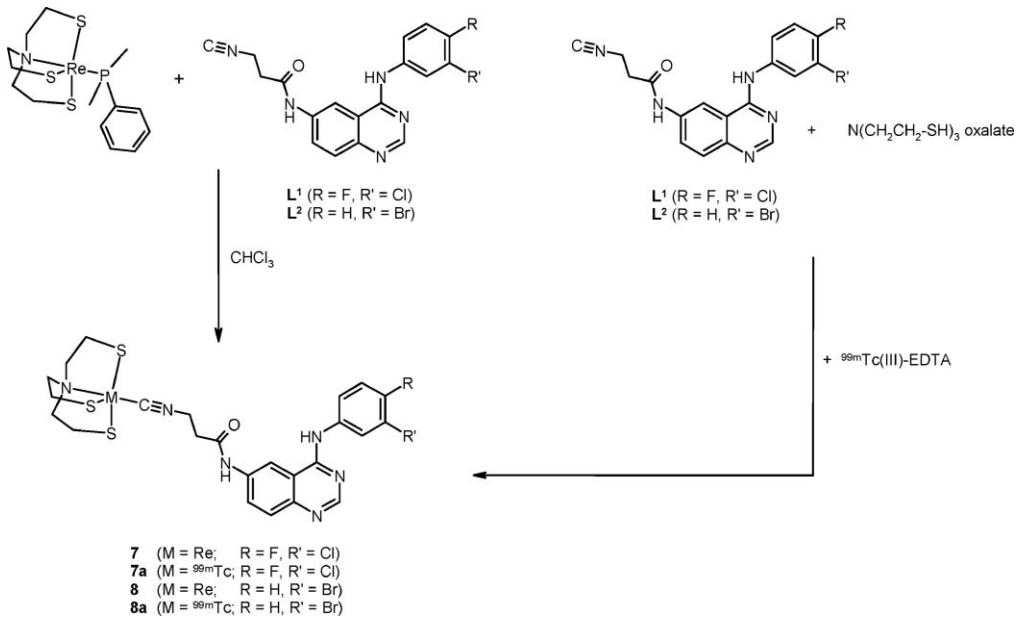

Scheme 2 Synthesis of M^{III} complexes (M = Re,**7**, **8**; ^{99m}Tc, **7a**, **8a**).

complexes **7** and **8** were formed by addition of the appropriate isocyanide ligands. The characterization of these complexes was based on ES/MS, IR, elemental analysis, NMR and, in the case of **8**, by X-ray diffraction analysis.

An ORTEP drawing of **8** is shown in Fig. 1, and the most relevant bond distances and angle are presented in Table 2. The complex adopts the trigonal-bipyramidal (tbp) geometry with the trigonal plane formed by the three thiolate sulfurs of the tripodal ligand. The central nitrogen atom of the chelate ligand and the monodentate isocyanide bearing the quinazoline moiety occupy the apical positions. The Tc–$S_{thiolato}$ distances are restricted in a narrow range (2.234(3)–2.249(4) Å) and compare well with those previously reported for trigonal bipyramidal [Tc(NS_3)(CN-R)]-type complexes.[33] This applies accordingly for the Re–C7 distance of 1.94 Å. The N1–Re–C7 axis shows only slight deviation from linearity (177.3°). Also the other angles of the inner coordination sphere are consistent with the tbp arrangement.

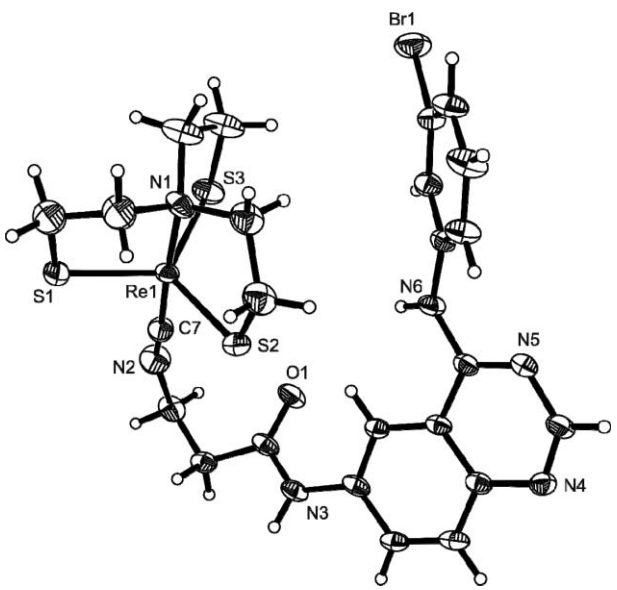

Fig. 1 ORTEP view of **8** with thermal ellipsoids drawn at 30% probability level.

The IR spectra of the Re reference complexes **7** and **8** exhibit a strong and very broad band in the 1950–1960 cm^{-1} range indicating the coordination of the isocyanide group. This band is significantly shifted to lower energies relatively to the corresponding free ligands $\mathbf{L^1}$ and $\mathbf{L^2}$ (Δ = 199 cm^{-1}, **7**; Δ = 202 cm^{-1}, **8**), indicating significant π-back donation from the metal to the isonitrile ligands.

The "4 + 1" ^{99m}Tc mixed-ligand complexes **7a** and **8a** were obtained in a two-step reaction (Scheme 2). In the first step $^{99m}Tc^{III}$-EDTA was formed by reduction of $^{99m}TcO_4^-$ (generator eluate) in Na_2EDTA solution. In the second reaction step the EDTA was substituted by the tripodal ligand tris(2-mercaptoethyl)amine and the appropriate monodentate isocyanide ($\mathbf{L^1}$, $\mathbf{L^2}$) resulting in the formation of the desired "4 + 1" ^{99m}Tc complexes (**7a**, **8a**). The yields obtained by this procedure were between 50 and 70%. The complexes presented high radiochemical purity after HPLC purification. The ^{99m}Tc complexes and the analogous Re complexes exhibited identical retention times in RP-HPLC investigations.

Previous studies have also shown that the *fac*-$[M(CO)_3]^+$ moiety can be stabilized by chelators with different denticities and/or donor atom sets.[36] We and others have used mainly tridentate chelators and we have shown the robustness of these complexes as well as their suitability for labelling different biomolecules.[24,36–43] To evaluate the effect of the metal fragment on the biological properties of the quinazoline pharmacophore, we have synthesized and characterized monoanionic and potentially tridentate chelators with a N_2O donor atom set and studied their suitability for labelling quinazoline fragments with the *fac*-$[M(CO)_3]^+$ moiety. One of the chelators has a pyrazolyl unit ($\mathbf{L^3}$H) and the other has a pyridine moiety ($\mathbf{L^6}$H). The pyrazolyl-containing ligand $\mathbf{L^3}$H was prepared by refluxing *N*-(2-bromoethyl)-3,5-dimethylpyrazole with glycine in water–ethanol (1 : 1) during 4 days, while maintaining the pH between 8 and 10. As can be seen in Scheme 3,

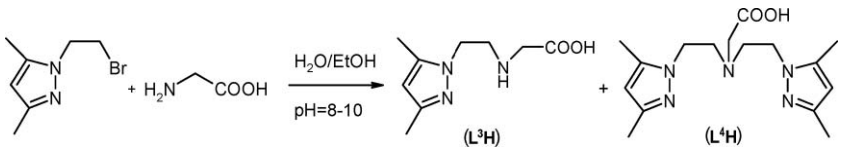

Scheme 3 Synthesis of $\mathbf{L^3}$H.

during the formation of $\mathbf{L^3}$H the symmetric pyrazolyl containing chelator $\mathbf{L^4}$H is also formed. The yield of $\mathbf{L^3}$H is maximized up to 80% by using a five-fold excess of glycine. Compound $\mathbf{L^3}$H was purified by chromatography and its characterization was based on spectroscopic data.

Before conjugation of the novel chelator $\mathbf{L^3}$H to the quinazoline fragment, its coordination capability towards *fac*-[Re(CO)$_3$] moiety was studied. As can be seen in Scheme 4, $\mathbf{L^3}$H reacts with [NEt$_4$]$_2$[Re(Br)$_3$(CO)$_3$] in water, in a 1 : 2 molar ratio, yielding the neutral complex [Re(κ^3-$\mathbf{L^3}$)(CO)$_3$], (**9**). Single crystals suitable for X-ray crystallography were obtained by slow concentration of a solution of the complex in water.

An ORTEP drawing of **9** is shown in Fig. 2, and the most relevant bond distances and angles are presented in Table 2. The complex adopts a distorted octahedral coordination geometry. The Re$^{\mathrm{I}}$ is coordinated to three carbonyls in a facial arrangement, the three remaining coordination positions being occupied by the oxygen atom of the carboxylate group and by the two nitrogen atoms of the pyrazolyl ring and secondary amine.

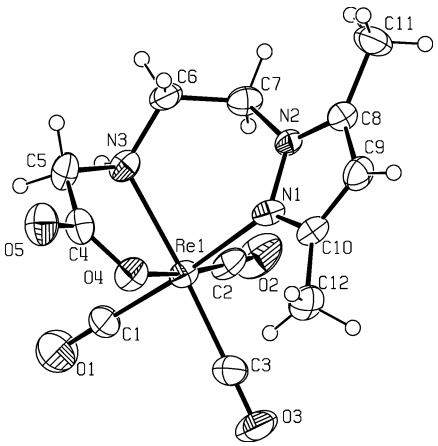

Fig. 2 ORTEP view of molecule 1 of **9** with thermal ellipsoids drawn at 30% probability level.

The IR spectrum of **9** displays two very strong ν(CO) bands in the 2021–1883 cm^{-1} range, confirming the *fac*-coordination geometry found in the solid state. The presence in this spectrum of a very strong band at 1627 cm^{-1} confirms the coordination of the oxygen atom of the carboxylic group to the metal center ($\Delta\nu$(C=O) = 25 cm^{-1} relative to the free ligand). In the ^{1}H NMR spectrum of **9** the resonances due to the pyrazolyl ring, as well as the resonances due to the ethylenic and methylenic groups, are downfield shifted compared to the free ligand $\mathbf{L^3}$H. Also, due to the tridentate coordination mode of $\mathbf{L^3}$ the hydrogen atoms of the ethylenic and methylenic groups become diastereotopic. In the ^{13}C NMR spectrum of **9** the three resonances due to the carbonyl groups appear at 196.4, 196.2 and 195.8 ppm, whereas the carbon of the carboxylate appears at 182.8 ppm. The latter is significantly downfield shifted relative to the same frequency in $\mathbf{L^3}$H ($\Delta\delta$ = 9.1 ppm), in agreement with the increase found in ν(CO).

At the ^{99m}Tc level, the [^{99m}Tc(κ^3-$\mathbf{L^3}$)(CO)$_3$] complex (**9a**) was obtained by reacting the *fac*-[^{99m}Tc(CO)$_3$(H$_2$O)$_3$]$^+$ (**1a**) with an aliquot of $\mathbf{L^3}$H in water, at 100 °C for 30 min, at pH 7.4. Complex **9a** was obtained almost quantitatively (>95%) even with very low concentration of $\mathbf{L^3}$H (10^{-5} M). The identity of **9a** (retention time (r.t.) = 16.0 min) was established by comparing the retention time in the HPLC radiochromatogram with the UV/Vis trace of the corresponding non-radioactive Re congener **9** (r.t. = 15.9 min). Complex **9a** is stable against histidine and cysteine challenge, and is also stable in human serum at 37 °C and presents low protein binding (<8%, 15 min–4 h incubation time at 37°C). Based on these results, a pyrazolyl-containing chelator bearing a quinazoline fragment ($\mathbf{L^5}$H) was synthesized and characterized and used to be labelled with the technetium tricarbonyl. Compound $\mathbf{L^5}$H was obtained by alkylation of the secondary amine of $\mathbf{L^3}$H with the quinazoline derivative, *N*-[4-[(3-chloro-4-fluorophenyl)amino]quinazolin-6-yl]bromopropionamide (**6**) (Scheme 5).

Compound $\mathbf{L^5}$H reacts with *fac*-[M(X)$_3$(CO)$_3$]$^{2-/+}$ yielding complexes *fac*-[M(κ^3-$\mathbf{L^5}$)(CO)$_3$] (M = Re, **10**; ^{99m}Tc, **10a**; Scheme 4).

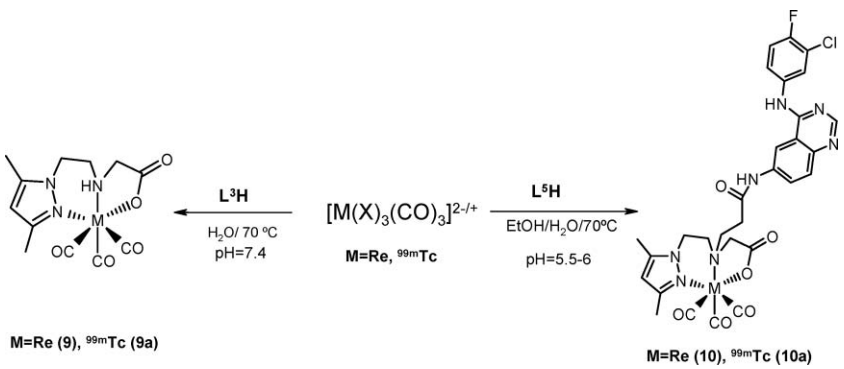

Scheme 4 Synthesis of **9**/**9a** and **10**/**10a**.

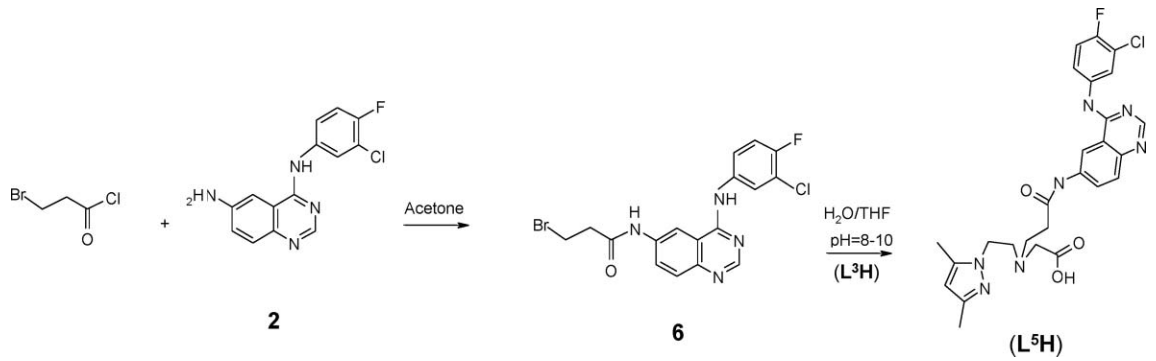

Scheme 5 Synthesis of **6** and $\mathbf{L^5}$H.

Unlike **9a**, the functionalized complex [^{99m}Tc(κ^3-$\mathbf{L^5}$)(CO)$_3$] (**10a**) can only be obtained quantitatively (>95%) and with high specific activity when the pH is adjusted to 5.5–6. At pH = 7.4, the value normally used for preparing ^{99m}Tc tricarbonyl complexes, **10a** was formed but in a relatively low yield (30%), due to competitive formation of **9a** (70%). The presence of **9a** is due to the hydrolysis of $\mathbf{L^5}$ at the C–N bond at pH = 7.4, during the labelling reaction, which is relatively uncommon. However, **10a** when formed at a lower pH can be left for several hours in PBS (phosphate-buffered saline, pH 7.4, 37 °C), or in the presence of excess histidine or cysteine, without any hydrolysis to **9a** and/or transchelation.

As indicated in Scheme 6, compound $\mathbf{L^6}$H was prepared by reacting picolylaminodiacetic acid with *N*,*N*-bis[2-oxo-3-oxazolidinyl]phosphorodiamidic chloride in the presence of triethylamine and using THF as solvent. The picolylaminodiacetic anhydride formed reacts with 6-amino-4-[(3-bromophenyl)amino]quinazoline (**3**) in THF. The final compound $\mathbf{L^6}$H was obtained after evaporation of the solvent and purification of the crude by chromatography on silica gel. This compound obtained in relatively high yield, was characterized by NMR, IR spectroscopy and elemental analysis. The reactions with the *fac*-[M(CO)$_3$(H$_2$O)$_3$]$^{2-/+}$ yielded complexes *fac*-[M(κ^3-$\mathbf{L^6}$)(CO)$_3$] (M = Re, **11**; ^{99m}Tc, **11a**). The ^{99m}Tc complex **11a** was found to be stable for several hours in PBS (pH 7.4, 37 °C), or in the presence of excess histidine or cysteine. The Re complexes, **10** and **11**, were characterized by the normal techniques in inorganic chemistry, and were used as surrogates for the characterization of the analogous ^{99m}Tc complexes, **10a** and **11a**, by HPLC.

Cellular inhibition activities—*in vitro* screening

The ligands ($\mathbf{L^1}$, $\mathbf{L^2}$, $\mathbf{L^5}$H, $\mathbf{L^6}$H) as well as the rhenium complexes (**7**, **8**, **10**, **11**) were evaluated for their potency to inhibit EGFR autophosphorylation using intact A431 cells. All the compounds were found to be potent inhibitors, their IC$_{50}$ values being below 1 μM (Table 3), indicating that they have crossed the cell membrane (Fig. 3). So far, due to the limited number of compounds available, a detailed structure–activity relationship is difficult to determine, although some indications can be outlined. Functionalization of the 6-amino group of the parent compounds (**2**, **3**) with the isocyano group *via* a C$_3$ alkyl amide linker ($\mathbf{L^1}$, $\mathbf{L^2}$, respectively) resulted in the most potent ligands of the series. $\mathbf{L^5}$H and $\mathbf{L^6}$H showed lower potency compared to $\mathbf{L^1}$ and $\mathbf{L^2}$ respectively. This can be attributed to the ionization of their COOH group that lessens the penetration of cell membrane.

The incorporation of the rhenium cores ReNS$_3$ and Re(CO)$_3$ does not decrease dramatically the potency of the corresponding ligands. Among the complexes tested compound **8** is the most potent, even more potent than all the other ligands ($\mathbf{L^1}$, $\mathbf{L^5}$H, $\mathbf{L^6}$H).

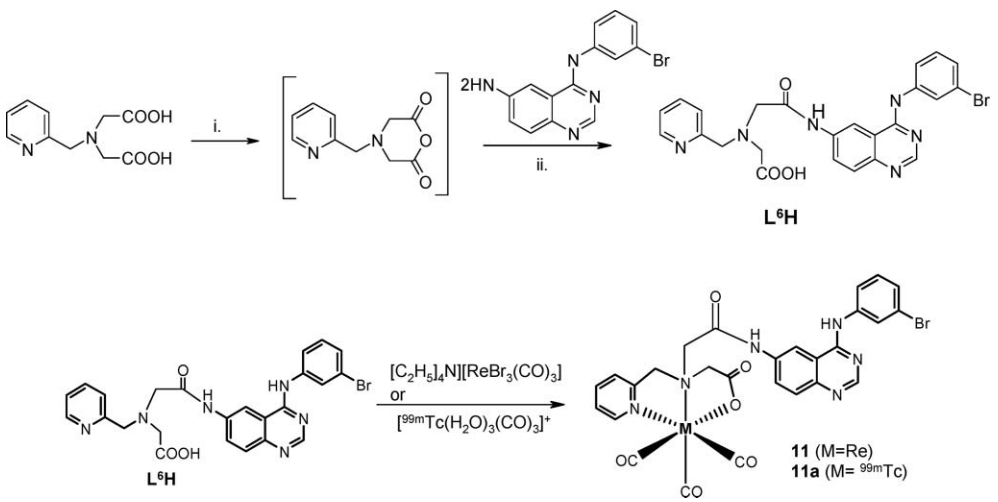

Scheme 6 Synthesis of $\mathbf{L^6}$H and of *fac*-[M(κ^3-$\mathbf{L^6}$)(CO)$_3$] (M = Re, **11**; ^{99m}Tc, **11a**): i BOP-Cl, Et$_3$N, THF, 20 °C; ii THF, RT.

Table 3 Inhibition of EGFR tyrosine kinase and A431 cell growth by quinazolines and their rhenium complexes

Compound	Inhibition of autophosphorylation IC_{50}/nM[a]	Inhibition of cell Growth IC_{50},/μM[b]
L[1]	130 ± 39	4.2 ± 0.9
7	481 ± 20	6.4 ± 1.8
L[2]	72 ± 3	2.9 ± 0.3
8	108 ± 13	2.9 ± 1.6
L[5]H	236 ± 31	2.1 ± 1.1
10	331 ± 27	7.3 ± 1.2
L[6]H	545 ± 33	23.8 ± 5.1
11	756 ± 137	41.2 ± 13.6
2	4.6 ± 1.3	4.2 ± 0.2
3	3.5 ± 1.1	4.8 ± 0.2

[a] Concentration (nM) needed to inhibit by 50% the autophosphorylation of EGFR in A431 cells (detected by immunoblotting). [b] Dose-response curves were determined at six concentrations. The IC_{50} values are the concentration (μM) needed to inhibit cell growth by 50%. IC_{50} values for each derivative were obtained from three independent experiments and are represented as mean ± standard deviation. Each experiment was performed in duplicate in the case of inhibition of autophosphorylation and in quadruplicate in the case of inhibition of cell growth.

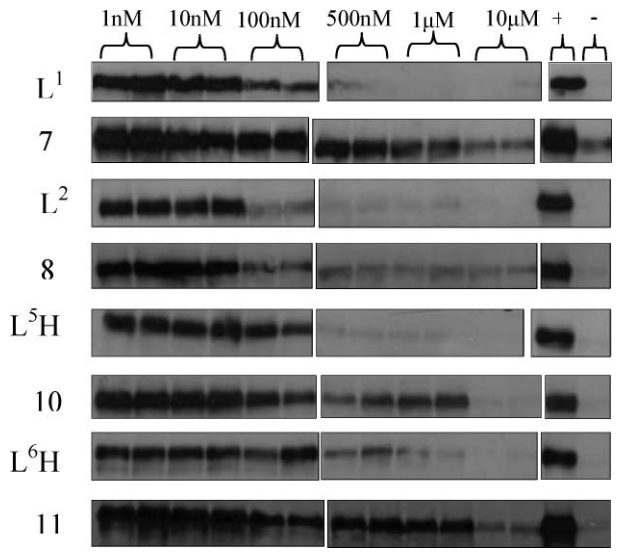

Fig. 3 Inhibition of EGFR autophosphorylation in intact A431 cells. Cells were incubated with **L**[1], **7**, **L**[2], **8**, **L**[5]H, **10**, **L**[6]H, **11** at concentrations ranging from 1 nM to 10 μM and then stimulated with EGF. Whole cell lysates were Western blotted using antiphosphotyrosine antibody.

The ligands (**L**[1], **L**[2], **L**[5]H, **L**[6]H) as well as the rhenium complexes (**7**, **8**, **10**, **11**) were also evaluated for their potency to inhibit the growth of A431 cells. Most of the compounds tested were found to be potent inhibitors, with IC_{50} values below 10 μM (Table 3). Among the compounds studied, **L**[5]H is the most potent. Generally, the potency of the other compounds follows the potency of autophosphorylation test.

Concluding remarks

Searching for useful ^{99m}Tc probes for early detection and staging of EGFR positive tumors, we have coupled two quinazoline pharmacophores to tailor-made chelators suitable for the stabilization of the "4 + 1" mixed-ligand system $[M(NS_3)(CN\text{-}R)]$ and the tricarbonyl moiety *fac*-$[M(CO)_3]^+$. The tailor-made bifunctional chelators allowed the ^{99m}Tc labeling of the quinazoline fragments in high yield and with high radiochemical purity. The nature and structure of the radioactive complexes were established by comparing their HPLC profiles with those of the corresponding Re surrogates, which were fully characterized by normal analytical techniques, including by X-ray diffraction analysis, in the cases of complexes **8** and **9**. The radioactive complexes are quite stable to oxidation and/or transchelation in physiological media. *In vitro* studies have shown that the quinazoline fragments after conjugation to an isocyanide monodentate ligand or to a pyrazolyl-containing tridentate chelator as well as the corresponding metal complexes are still able to cross the cell membrane of A431 cells inhibiting significantly the EGFR autophosphorylation and cell growth. These two effects were also found for the pyridine-containing chelator and for the corresponding metal complex, although to a lesser extent. To the best of our knowledge, the work described in this article is the first attempt to target the intracellular part of EGFR with a quinazoline fragment coordinated to a metal center, through bifunctional chelators tailor-made to stabilize Re and Tc^{III} and Tc^{I}. Based on these findings biodistribution studies with ^{99m}Tc complexes in healthy and tumor-bearing mice are currently in progress to prove their usefulness as tumor imaging agents.

Acknowledgements

This project was part of an IAEA Coordinated Research Project "Development of ^{99m}Tc-based small bio-molecules using novel ^{99m}Tc cores". Special thanks go to D. V. S. Narasimhan and M. R. A. Pillai of the Department of Nuclear Sciences and Applications of the IAEA, for their efforts in the success of this Coordinated Research Project.

References

1 J. J. Laskin and A. B. Sandler, *Cancer Treat. Rev.*, 2004, **30**, 1–17.
2 R. Bianco, T. Gelardi, V. Damiano, F. Ciardiello and G. Tortora, *Int. J. Biochem. Cell Biol.*, 2007, **39**, 1416–1431.
3 R. Zandi, A. B. Larsen, P. Andersen, M.-T. Stockhausen and H. S. Poulsen, *Cell. Signalling*, 2007, **19**, 2013–2023.
4 C. Arteaga, *Semin. Oncol.*, 2003, **30/7**, 3–14.
5 C. A. Ritter and C. Arteaga, *Semin. Oncol.*, 2003, **30/1**, 3–11.
6 R. D. Mass, *Int. J. Radiat. Oncol., Biol., Phys.*, 2004, **58**, 932–940.
7 J. Albanell and P. Gascón, *Curr. Drug Targets*, 2005, **6**, 259–274.
8 D. Vallböhmer and H.-J. Lenz, *Clin. Colorectal Cancer*, 2005, (Suppl. 5), S19–S27.
9 W. Cai, G. Niu and X. Chen, *Eur. J. Nucl. Med. Mol. Imaging*, 2008, **35**, 186–208.
10 P. Johnström, A. Fredriksson, J. O. Thorell and S. Stone-Elander, *J. Labelled Compd. Radiopharm.*, 1998, **41**, 623–629.
11 I. Ben-David, Y. Rozen, G. Ortu and E. Mishani, *Appl. Radiat. Isot.*, 2003, **58**, 209–217.
12 E. Mishani, G. Abourbeh, Y. Rozen, O. Jacobson, D. Laky, I. Ben, David, A. Levitzki and M. Shaul, *Nucl. Med. Biol.*, 2004, **31**, 469–476.
13 A. Fredriksson, P. Johnström, J.-O. Thorell, G. von Heijne, M. Hassan, S. Eksborg, P. Kogner, P. Borgstöm, M. Ingvar and S. Stone-Elander, *Life Sci.*, 1999, **65**, 165–174.
14 J.-Q. Wang, M. Gao, K. D. Miller, G. W. Sledge and Q.-H. Zheng, *Bioorg. Med. Chem. Lett.*, 2006, **16**, 4102–4106.
15 E. Samén, J.-Q. Thorell, A. Fredriksson and S. Stone-Elander, *Nucl. Med. Biol.*, 2006, **33**, 1005–1011.
16 E. Mishani, G. Abourbeh, O. Jacobson, S. Dissoki, R. B. Daniel, Y. Rozen, M. Shaul and A. Levitzki, *J. Med. Chem.*, 2005, **48**, 5337–5348.
17 G. Ortu, I. Ben-David, Y. Rozen, N. M. T. Freedman, R. Chisin, A. Levitzki and E. Mishani, *Int. J. Cancer*, 2002, **101**, 360–370.

18 T. A. Bonasera, G. Ortu, Y. Rozen, R. Krais, N. M. Freedman, R. Chisin, A. Gazit, A. Levitzki and E. Mishani, *Nucl. Med. Biol.*, 2001, **28**, 359–374.
19 Y. Seimbille, M. E. Phelps, J. Czernin and D. H. S. Silverman, *J. Labelled Compd. Radiopharm.*, 2005, **48**, 829–843.
20 S. Dissoki, Y. Aviv, D. Laky, G. Abourbeh, A. Levitzki and E. Mishiani, *Appl. Radiat. Isot.*, 2007, **65**, 1140–1151.
21 G. Abourbeh, S. Dissoki, O. Jacobson, A. Litchi, R. B. Daniel, D. Laki, A. Levitzki and E. Mishani, *Nucl. Med. Biol.*, 2007, **34**, 55–70.
22 M. Shaul, G. Abourbeh, O. Jacobson, Y. Rozen, L. Desideriu, A. Levitzki and E. Mishani, *Bioorg. Med. Chem.*, 2004, **12**, 3421–3429.
23 A. Pal, A. Glekas, M. Doubrovin, J. Balatoni, T. Beresten, D. Maxwell, S. Soghomonyan, A. Shavrin, L. Ageyeva, R. Finn, S. M. Larson, W. Bornmann and J. G. Gelovani, *Mol. Imaging Biol.*, 2006, **8**, 262–277.
24 S. Alves, A. Paulo, J. D. G. Correia, Â. Domingos and I. Santos, *J. Chem. Soc., Dalton Trans.*, 2002, 4714–4719.
25 E. R. Shepherd, A. M. Sweetland and E. D. Junker, *J. Inorg. Biochem.*, 1997, **65**, 1–14.
26 J. Cabre-Castellvi, A. Palomo-Coll and A. L. Palomo-Coll, *Synthesis*, 1981, 616–620.
27 J. F. Smaill, B. D. Palmer, G. W. Rewcastle, W. A. Denny, D. J. McNamara, E. M. Dobrusin, A. J. Bridges, H. Zhou, H. D. Showalter, R. T. Winters, W. R. Leoplod, D. W. Fry, J. M. Nelson, V. Slintak, W. L. Elliot, B. J. Roberts, P. W. Vincent and S. J. Patmore, *J. Med. Chem.*, 1999, **42**, 1803–1815.
28 G. W. Rewcastle, W. A. Denny, A. Bridges, H. Zhou, D. R. Cody, A. McMichael and D. W. Fry, *J. Med. Chem.*, 1995, **38**, 3482–3487.
29 H. Spies, M. Glaser, H.-J. Pietzsch, F. E. Hahn and T. Lügger, *Inorg. Chim. Acta*, 1995, **240**, 465–478.
30 R. Alberto, R. Schibli, A. Egli and P. A. Schubiger, *J. Am. Chem. Soc.*, 1998, **120**, 7987–7988.
31 L. J. Ferrugia, *J. Appl. Crystallogr.*, 1999, **32**, 837.
32 L. J. Ferrugia, *J. Appl. Crystallogr.*, 1997, **30**, 565.
33 H.-J. Pietzsch, A. Gupta, R. Syhre, P. Leibnitz and H. Spies, *Bioconjugate Chem.*, 2001, **12**(4), 538–544.
34 S. Seifert, J.-U. Künstler, E. Schiller, H.-J. Pietzsch, B. Pawelke, R. Bergmann and H. Spies, *Bioconjugate Chem.*, 2004, **15**(4), 856–863.
35 M. Walther, C. M. Jung, R. Bergmann, J. Pietzsch, K. Rode, K. Fahmy, P. Mirtschink, S. Stehr, A. Heintz, G. Wunderlich, W. Kraus, H.-J. Pietzsch, J. Kropp, A. Deußen and H. Spies, *Bioconjugate Chem.*, 2007, **18**, 216–230.
36 R. Alberto, *Top. Curr. Chem.*, 2005, **252**, 1–44.
37 I. Santos, A. Paulo and J. D. G. Correia, *Top. Curr. Chem.*, 2005, **252**, 45–84.
38 S. Alves, J. D. G. Correia, L. Rold, A. Prasanphanich, R. Haubner, M. Rupprich, E. von Guggenberg, R. Alberto, C. Decristoforo, I. Santos and C. J. Smith, *Bioconjugate Chem.*, 2007, **18**, 530–537.
39 R. Garcia, L. Gano, L. Maria, A. Paulo, I. Santos and H. Spies, *JBIC, J. Biol. Inorg. Chem.*, 2006, **11**, 769–782.
40 L. Maria, A. Paulo, I. C. Santos, I. Santos, P. Kurz, B. Spingler and R. Alberto, *J. Am. Chem. Soc.*, 2006, **128**, 14590–14598.
41 S. Tzanopoulou, I. C. Pirmettis, G. Patsis, M. Paravatou-Petsotas, E. Livaniou, M. Papadopoulos and M. Pelecanou, *J. Med. Chem.*, 2006, **49**, 5408–5410.
42 C. Müller, A. Hohn, P. A. Schubiger and R. Schibli, *Eur. J. Nucl. Med. Mol. Imaging*, 2006, **33**, 1007–1016.
43 B. Spingler, S. Mundwiler, P. Ruiz-Sánchez, R. D. van Staveren and R. Alberto, *Eur. J. Inorg. Chem.*, 2007, 2641–2647.